

# RSC Advances



This is an *Accepted Manuscript*, which has been through the Royal Society of Chemistry peer review process and has been accepted for publication.

*Accepted Manuscripts* are published online shortly after acceptance, before technical editing, formatting and proof reading. Using this free service, authors can make their results available to the community, in citable form, before we publish the edited article. This *Accepted Manuscript* will be replaced by the edited, formatted and paginated article as soon as this is available.

You can find more information about *Accepted Manuscripts* in the [Information for Authors](#).

Please note that technical editing may introduce minor changes to the text and/or graphics, which may alter content. The journal's standard [Terms & Conditions](#) and the [Ethical guidelines](#) still apply. In no event shall the Royal Society of Chemistry be held responsible for any errors or omissions in this *Accepted Manuscript* or any consequences arising from the use of any information it contains.

# Selectively Detecting of Trace Picric Acid by Reduced Perylene Bisimide with POSS Substituents and Their Nanoaggregates

Cite this: DOI: 10.1039/x0xx00000x

Bo Yu, Jiajun Ma, Yujuan Zhang, Gang Zou, Qijin Zhang\*

Received 00th January 2012,  
Accepted 00th January 2012

DOI: 10.1039/x0xx00000x

www.rsc.org/

Reduced perylene bisimides (PBIs) with two substituents of polyhedral oligomeric silsesquioxane (POSS) are designed and synthesized for rapid and selective detection of picric acid in THF solution. Nanoaggregates of the reduced PBI show fluorescence that is also sensitive to the concentration change of picric acid.

## Introduction

Picric acid (PA) has become a significant environmental pollutant because it has been widely used in the leather, pharmaceutical, and dye industries, as well as in the manufacture of explosive and rocket fuels, but it is also a strong irritant and allergen.<sup>1</sup> Under this circumstance, many methods for detection of PA have been developed, in which fluorescence sensors show more advantages in terms of sensitivity, selectivity, simplicity and real-time for the detection of PA.<sup>2,3</sup> The already existing materials for the fluorescence sensors include organic conjugated polymers<sup>4</sup> or polymer composite film<sup>1</sup> and metal-organic framework.<sup>5</sup> All of them exhibit a fluorescent response to PA, likely through a host-guest interaction combined with an electron transfer process from the electron-rich fluorophore to the electron-deficient PA.<sup>2,6</sup>

On the other hand, solid-state fluorescence sensing has received considerable attention.<sup>7,8</sup> Effective solid aggregate fluorescence sensors based on organic materials are often demanding available organic substances that exhibit strong fluorescence in the solid state and suitable binding or absorption sites that can capture the analyte molecules.<sup>9</sup> PBIs, for example, are often reported to detect aniline by modifying with substituent groups due to their strong  $\pi$ - $\pi$  stacking and solid fluorescence.

PBIs have been extensively investigated as organic dyes due to their high molar absorptivity, high quantum yields of fluorescence with excellent photochemical and thermo-stability.<sup>10</sup> Out of near-unity fluorescence quantum yields in solutions, as suitable luminophore in fluorescence sensors PBIs' derivatives are often designed and synthesized by two approaches: one is prolonging their main chains<sup>11-13</sup> and the other is modifying their bay-substituents.<sup>14,15</sup> Both of them are heavy workload and for the second method, the bay-substituted groups hinder the  $\pi$ - $\pi$  stacking.

In this paper, a new strategy is proposed to extend sensor applications of PBIs, in which PBI is used as backbone and POSS as substituents to form organic-inorganic hybrid fluorescent molecules (**PDP-1**). The intramolecular organic-inorganic hybrid structure endows PBI with extraordinary properties such as excellent thermal stability and solubility, a low dielectric constant and an outstanding oxygen plasma etching resistance.<sup>16</sup> Reduction of the carbonyl groups in **PDP-1** is used to derive **PDP-2** (shown in Fig. 1) with the strong electron-rich tertiary nitrogen centre, which has strong response to electron-deficient molecule such as PA and is prone to form hydrogen bonds with the hydroxyl of PA in aprotic solvents, resulting in much more interactions between **PDP-2** and PA than other electron-deficient molecules.

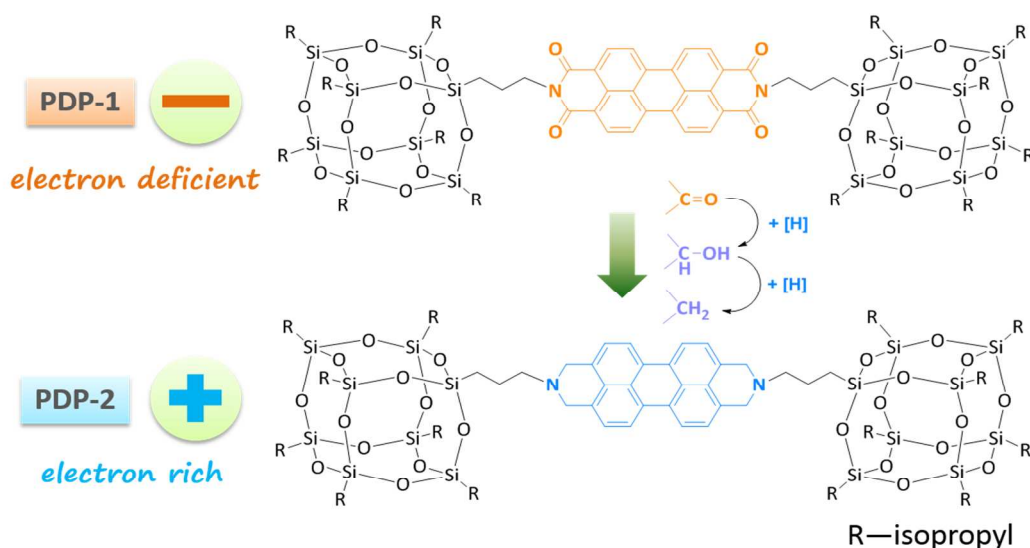


Fig.1 Molecular formula of the PDP-1 and PDP-2 and the synthetic mechanism from PDP-1 to PDP-2.

## Results and Discussion

From UV–vis spectra of **PDP-1** and **PDP-2** in THF shown in Fig.2a, it can be seen that the maximum absorption peaks of two samples are located at 525nm and 460nm, respectively. Compared with the absorption of PA (black line in Fig.2a), it is easily found that the absorption band of PA has sensible overlap with the absorption of **PDP-2**, other than that of **PDP-1**, because there is a blue shift of 65nm between two absorptions of **PDP-1** and **PDP-2**. Under irradiation of light at 445 nm, **PDP-2** has strong fluorescence at about 460 nm that is overlapped with the absorption of PA (Fig.2b). From the results of the previous research for the detection of PA, it is known that the fluorescence quenching of **PDP-2** might occur due to the possible formation of non-fluorescent complex when there is an interaction between PA containing strong electron-withdrawing groups and **PDP-2** with strong electron-rich tertiary nitrogen.<sup>2</sup> This expectation has been verified by experimental results shown in Fig.3: by gradually adding PA solution of 18 $\mu$ M to the solution of 1.5 $\mu$ M **PDP-2** in THF the fluorescence quenching is observed (the result has been corrected for the dilution introduced by the addition of the PA solution) (Fig.3a). The mechanism about this fluorescence quenching is caused by interaction between PA and **PDP-2** as shown in Fig.3c, similar to the description in the reported work.<sup>17</sup> Detailed information concerning this interaction can be

obtained from the change of <sup>1</sup>H NMR before and after adding trace PA, in which the resonant peak of the methylene linking with tert-nitrogen group is shifted downfield from 3.02 to 3.39 ( $\Delta\sigma=0.37$ ) (Fig.S4) and the decrease in the fluorescence lifetime of **PDP-2** in mixture solution (Fig.S5) also imply there is energy transfer between **PDP-2** and PA. Results shown in Fig.3b have obviously testified that the quenching course agrees with the Stern-Volmer plot. The detection limit ( $3\sigma/\text{slope}$ ) of PA is calculated at least down to 80nM. In addition, the fluorescence quenching of **PDP-2** with the addition of PA can also be observed by the naked eye (Fig.S6), owing to the large Stern–Volmer data ( $K_{sv}=1.19 \times 10^6 \text{ L}\cdot\text{mol}^{-1}$ ) comparing with other turn-off sensors (Table S1).

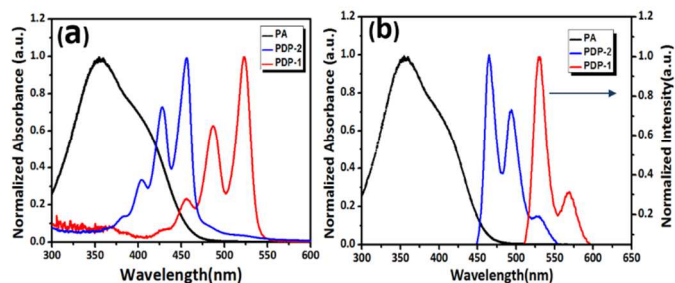
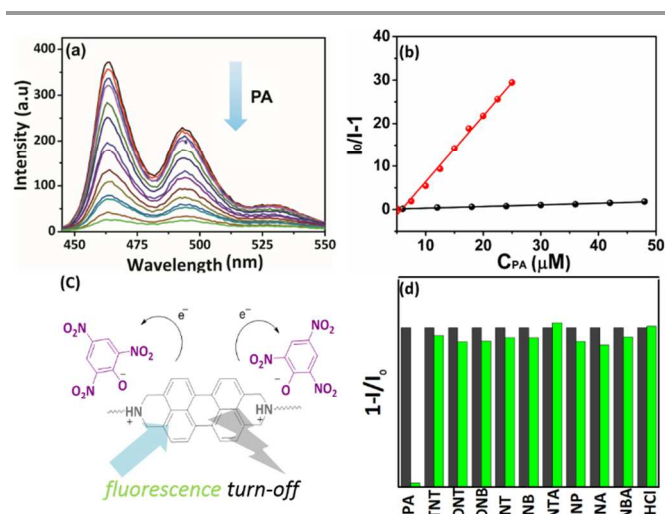


Fig.2 (a) Absorption spectra of **PDP-1** (red), **PDP-2** (blue) and PA (black) in THF solution. (b) Absorption spectrum of PA (black) and fluorescence spectra of **PDP-1** (red), **PDP-2** (blue) in THF with different excitation with wavelength at 500 nm for **PDP-1** and at 445 nm for **PDP-2**, respectively.

In order to investigate the **PDP-2**'s property of recognition of nitro aromatic compounds, the fluorescence

behaviour of **PDP-2** toward different nitro compounds: picric acid (PA), 2,4,6-trinitrotoluene (TNT), 2,4-dinitrotoluene (DNT), 1,4-dinitrobenzene (DNB), p-nitro-toluene (NT), p-nitrobenzene (NB), p-toluylicacid (NTA), p-nitrobenzoic acid (NA), p-nitrophenol (NP), and benzoic acid (NBA), are performed with the same concentration ( $2 \times 10^{-5} \text{ mol} \cdot \text{L}^{-1}$ ). Hydrochloric acid (HCl) is also used as a blank sample to eliminate the influence of the proton because the tertiary nitrogen is easily to interact with protons.



**Fig.3** (a) The change of fluorescence intensity of **PDP-2** with the addition of PA in THF, (b) the Stern–Volmer plot of quenching of different substituent groups of PBIs (red line stands for **PDP-2**, black line is **PDP-1**) (c) Quenching Mechanism of **PDP-2** with PA (d) Plots of  $1-I_0/I$  for PA and other nitroderivatives (black and green histograms respectively stand for the result before and after addition).

The response of the fluorescence emission of **PDP-2** in THF to PA, TNT, DNT, DNB, NT, NB, NTA, NP, NA, NBA and HCl is also well-established as shown in Fig.3d, in which it is found that no significant change in **PDP-2** fluorescence is observed by addition of equivalent amount of above nitro compounds, except PA (Fig.3d). Because of a lack of tendency to protonate the tert-nitrogen group of **PDP-2**, nitro derivatives other than PA do not follow the ionic mechanism, which reduces their quenching efficiencies of the fluorescence of **PDP-2**.

Solid **PDP-2** can be obtained by concentrating the solution of **PDP-2** in THF, however, there is no fluorescence observed in this solid state **PDP-2** (Fig.S7). This behaviour is different from that of similar structure of PBI with  $\beta$ -cyclodextrin as substituents.<sup>9</sup> In **PDP-2**, POSS substituent has a small volume that has no effect on the ordered arrangement of **PDP-2**, and fluorescence quenching would take place through energy transfer between ordered **PDP-2** as shown in Fig.S8.

In order to overcome this problem, nanoaggregates of **PDP-2** were prepared by interfacial assembly.<sup>18</sup> The morphology of the nanoaggregate has been observed by SEM as shown in Fig.4b.

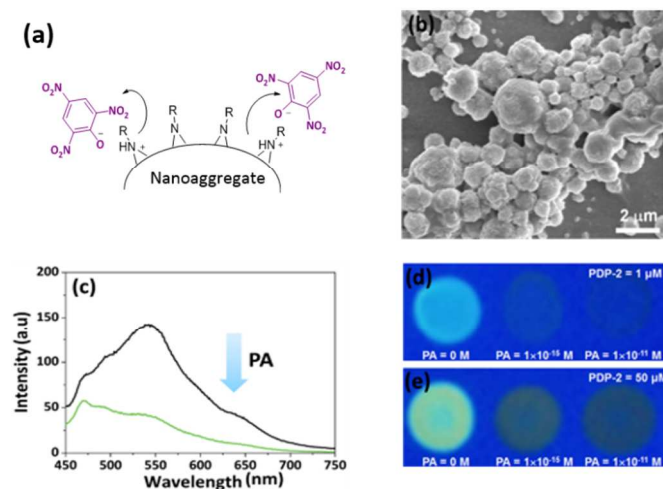


**Fig.4** (a) Quenching Mechanism of **PDP-2** with PA in solid state (b) The photo of aggregation state of **PDP-2** by SEM. (c) The detection curve of solid state **PDP-2** for PA. (d) The quenching demonstration of **PDP-2** (1  $\mu\text{M}$ ) in paper with addition PA 0,  $10^{-15}$  M,  $10^{-11}$  M, respectively and (e) **PDP-2** (50  $\mu\text{M}$ ) and with addition PA 0,  $10^{-15}$  M,  $10^{-11}$  M, respectively.

Comparing with the alkyl groups disubstituted PBIs, the fluorescence of the nanoaggregate of **PDP-2** can be observed due to the unique stacking effect of POSS. Furthermore, under an excitation of light at 445 nm, the maximum is located at about 550 nm as shown in Fig.4c, although the emission looks unlike that of **PDP-2** in THF solution. The possible reason for this phenomenon is that large specific surface makes the ordered arrangement of **PDP-2** loss, producing partly fluorescence quenching. In this way, it is expected that the tert-nitrogen group on the surface of nanoaggregates is still active to the PA molecules.

When a solution containing nanoaggregates of **PDP-2** is dropped onto the paper, the photoluminescence also exists as shown in Fig.4d. When the solution of PA is dropped onto the paper, the fluorescence quenching takes place as shown in Fig. 4(d) and 4(e), in which it is found that the detected concentration of PA is  $10^{-15}$  M in this way. This is a relatively low concentration for detecting PA in comparison with previous reported works.<sup>19</sup>

## Conclusions

In summary, reduced PBI with two POSS substituents (**PDP-2**) has been synthesized for detection of PA. **PDP-2**

solution in THF shows a selective, sensitive, colorimetric, and ratiometric fluorescent quenching to PA with  $K_{sv}$  to be  $1.19 \times 10^6 \text{ L}\cdot\text{mol}^{-1}$ . The fluorescent quenching to PA is lost in solid state of **PDP-2**, however, nanoaggregates of **PDP-2** prepared by interfacial assembly are found to have fluorescence that can be quenched by dropping PA solution in THF, and the lowest detection concentration is found to be  $10^{-15}\text{M}$ . As a general design strategy, reduced PBI with POSS substituents may allow us to create further fluorescent sensor candidates for PA in the future.

### Acknowledgements

This work is supported by National Natural Science Foundation of China (No. 21074123, 91027024, 51173176 and 51273186).

### Notes and references

† Bo Yu, Jiajun Ma, Yujuan Zhang, Gang Zou, Qijin Zhang, Key Laboratory of Soft Matter Chemistry, Key Laboratory of Optoelectronic Science and Technology, Department of Polymer Science and Engineering, University of Science and Technology of China, Hefei, Anhui 230026, P. R. China. E-mail: zqjm@ustc.edu.cn.

Electronic Supplementary Information (ESI) available: [details of any supplementary information available should be included here]. See DOI: 10.1039/c000000x/

1. G. He, H. Peng, T. Liu, M. Yang, Y. Zhang and Y. Fang, *J Mater Chem*, 2009, **19**, 7347-7353.
2. Y. Peng, A.-J. Zhang, M. Dong and Y.-W. Wang, *Chem Commun*, 2011, **47**, 4505-4507.
3. Y. Ma, H. Li, S. Peng and L. Wang, *Analytical Chemistry*, 2012, **84**, 8415-8421.
4. S. J. Toal and W. C. Trogler, *J Mater Chem*, 2006, **16**, 2871-2883.
5. K. S. Asha, K. Bhattacharyya and S. Mandal, *Journal of Materials Chemistry C*, 2014, **2**, 10073-10081.
6. N. Dey, S. K. Samanta and S. Bhattacharya, *ACS Applied Materials & Interfaces*, 2013, **5**, 8394-8400.
7. V. Bellon-Maurel, O. Orliac and P. Christen, *Process Biochemistry*, 2003, **38**, 881-896.
8. V. Bhalla, A. Gupta and M. Kumar, *Org Lett*, 2012, **14**, 3112-3115.
9. Y. Liu, K.-R. Wang, D.-S. Guo and B.-P. Jiang, *Advanced Functional Materials*, 2009, **19**, 2230-2235.
10. M. Franceschin, C. Bombelli, S. Borioni, G. Bozzuto, S. Eleuteri, G. Mancini, A. Molinari and A. Bianco, *New Journal of Chemistry*, 2013, **37**, 2166-2173.
11. N. Pasaogullari, H. Icil and M. Demuth, *Dyes Pigments*, 2006, **69**, 118-127.
12. L. Zhong, F. Xing, W. Shi, L. Yan, L. Xie and S. Zhu, *ACS Applied Materials & Interfaces*, 2013, **5**, 3401-3407.
13. A. Arulkashmir, B. Jain, J. C. John, K. Roy and K. Krishnamoorthy, *Chem Commun*, 2014, **50**, 326-328.
14. A. J. Jimenez, M.-J. Lin, C. Burschka, J. Becker, V. Settels, B. Engels and F. Wurthner, *Chemical Science*, 2014, **5**, 608-619.
15. H.-Y. Tsai, C.-W. Chang and K.-Y. Chen, *Tetrahedron Letters*, 2014, **55**, 884-888.
16. L. Wang, Y. Ishida, R. Maeda, M. Tokita and T. Hayakawa, *RSC Advances*, 2014, **4**, 34981-34986.
17. V. Vij, V. Bhalla and M. Kumar, *ACS Applied Materials & Interfaces*, 2013, **5**, 5373-5380.
18. J.-S. Hu, Guo, H.-P. Liang, L.-J. Wan, C.-L. Bai and Y.-G. GuoWang, *The Journal of Physical Chemistry B*, 2004, **108**, 9734-9738.
19. S. Kaur, V. Bhalla, V. Vij and M. Kumar, *Journal of Materials Chemistry C*, 2014, **2**, 3936-3941.